Brandon J. Walker[1]
Medical Engineering,
Morgridge Institute for Research,
330 N. Orchard Street,
Madison, WI 53715
e-mail: bwalker4@wisc.edu

Benjamin L. Cox
Medical Engineering,
Morgridge Institute for Research,
330 N. Orchard Street,
Madison, WI 53715
e-mail: bcox1@wisc.edu

Ulas Cikla
Neurological Surgery,
University of Wisconsin,
1111 Highland Avenue,
Madison, WI 53705
e-mail: cikla@neurosurgery.wisc.edu

Gabriel Meric de Bellefon
Grainger Institute for Engineering,
1550 Engineering Drive,
Madison, WI 53706
e-mail: mericdebelle@wisc.edu

Behzad Rankouhi
Department of Mechanical Engineering,
University of Wisconsin,
1513 University Avenue,
Madison, WI 53705
e-mail: rankouhi@wisc.edu

Leo J. Steiner
Medical Engineering,
Morgridge Institute for Research,
330 N. Orchard Street,
Madison, WI 53715;
Department of Biomedical Engineering,
University of Wisconsin,
1550 Engineering Drive,
Madison, WI 53706
e-mail: lsteiner3@wisc.edu

Puwadej Mahadumrongkul
Medical Engineering,
Morgridge Institute for Research,
330 N. Orchard Street,
Madison, WI 53715;
Department of Mechanical Engineering,
University of Wisconsin,
1513 University Avenue,
Madison, WI 53706
e-mail: mahadumrongk@wisc.edu

George Petry
Medical Engineering,
Morgridge Institute for Research,
330 N. Orchard Street,
Madison, WI 53715
e-mail: gpetry@morgridge.org

An Investigation Into the Challenges of Using Metal Additive Manufacturing for the Production of Patient-Specific Aneurysm Clips

Cerebral aneurysm clips are biomedical implants applied by neurosurgeons to re-approximate arterial vessel walls and prevent catastrophic aneurysmal hemorrhages in patients. Current methods of aneurysm clip production are labor intensive and time-consuming, leading to high costs per implant and limited variability in clip morphology. Metal additive manufacturing is investigated as an alternative to traditional manufacturing methods that may enable production of patient-specific aneurysm clips to account for variations in individual vascular anatomy and possibly reduce surgical complication risks. Relevant challenges to metal additive manufacturing are investigated for biomedical implants, including material choice, design limitations, postprocessing, printed material properties, and combined production methods. Initial experiments with additive manufacturing of 316 L stainless steel aneurysm clips are carried out on a selective laser melting (SLM) system. The dimensions of the printed clips were found to be within 0.5% of the dimensions of the designed clips. Hardness and density of the printed clips (213 ± 7 HV1 and 7.9 g/cc, respectively) were very close to reported values for 316 L stainless steel, as expected. No ferrite and minimal porosity is observed in a cross section of a printed clip, with some anisotropy in the grain orientation. A clamping force of approximately 1 N is measured with a clip separation of 1.5 mm. Metal additive manufacturing shows promise for use in the creation of custom aneurysm clips, but some of the challenges discussed will need to be addressed before clinical use is possible.
[DOI: 10.1115/1.4043651]

Keywords: 3D printing, metal additive manufacturing, aneurysm clip(s), patient-specific devices, medical devices, neurosurgery

[1]Corresponding authors.
Manuscript received January 15, 2019; final manuscript received April 9, 2019; published online July 15, 2019. Assoc. Editor: Kunal Mitra.

Mythili Thevamaran
Grainger Institute for Engineering,
1550 Engineering Drive,
Madison, WI 53706
e-mail: mthevamaran@wisc.edu

Rob Swader
Medical Engineering,
Morgridge Institute for Research,
330 N. Orchard Street,
Madison, WI 53715
e-mail: rswader@morgridge.org

John S. Kuo
Department of Neurosurgery and Mulva
Clinic for the Neurosciences,
Dell Medical School,
University of Texas at Austin,
1701 Trinity Street, Stop Z1500,
Austin, TX 78712
e-mail: john.kuo@austin.utexas.edu

Krishnan Suresh
Department of Mechanical Engineering,
University of Wisconsin,
1513 University Avenue,
Madison, WI 53706
e-mail: ksuresh@wisc.edu

Dan Thoma
Grainger Institute for Engineering,
1550 Engineering Drive,
Madison, WI 53706
e-mail: dthoma@wisc.edu

Kevin W. Eliceiri[1]
Medical Engineering,
Morgridge Institute for Research,
330 N. Orchard Street,
Madison, WI 53715;
University of Wisconsin,
1111 Highland Avenue,
Madison, WI 53705
e-mail: eliceiri@wisc.edu

Introduction

There is a hemorrhagic stroke risk of approximately 6–20 cerebral aneurysm ruptures per 100,000 person-years with a very high 50% mortality rate at 30 days postrupture. Even for surviving patients, they have a similar high incidence of residual neurological deficits [1]. Although aneurysms can arise from arteries anywhere in the body, they are most frequently found in brain vasculature with known primary risk factors including hypertension, alcohol abuse, smoking, and genetic predisposition [2]. Degeneration and weakening of the walls of a cerebral artery, especially at high pressure branch points, results in bulging and formation of an aneurysm that can subsequently rupture and cause a large hemorrhagic stroke [3]. A costly but proven classical treatment for aneurysms (diagnosed with imaging or after initial rupture) to prevent devastating stroke is neurosurgical application of aneurysm clips. Some of the factors contributing to the associated high costs are derived from the critical function these devices serve and a laborious manufacturing process. Highly trained complex neurosurgical skills are required intraoperatively to adapt the current repertoire of standard clips to adequately treat variable vascular anatomy, whereas presurgical patient-specific customization of clips would potentially increase surgical efficacy and reduce operative risks.

In aneurysm clipping, a small metal clip is used to isolate the weakened wall of the aneurysm from normal blood circulation by re-approximating arterial vessel walls. Temporary clips are most often used to perform intermediate tasks (such as temporary upstream vessels to reduce hemorrhagic risk) during surgery and are removed prior to the end of an operation [4]. For example, a

Fig. 1 An example Yasargil aneurysm clip is shown with curved blades

parent artery may need to be temporarily occluded prior to the main aneurysm occlusion, to permit exploration of the aneurysm "neck" (connection of the aneurysm to the artery), possible aneurysm manipulation to discern surrounding vascular anatomy and connections and to determine the best strategy for safe aneurysm clipping without occluding blood flow in adjacent vessels. Sometimes aneurysms incorporate adjacent vessels, and therefore, the aneurysm needs to be clipped in multiple steps or only partially occluded. Other times, atherosclerosis prevents straightforward vessel wall reconstruction with standard clips and a creative or optimal clipping solution must be envisioned under the intraoperative time pressure with a limited repertoire of clips. In addition, permanent clips remain in a patient's brain after a procedure is completed and must be extremely biocompatible as well as consistent in strength over the remaining lifetime.

There are several important attributes to a properly functioning permanent aneurysm clip. The strength of the clip closing force is vital for ensuring the occlusion is successful, with temporary clips typically having a lighter 0.8 N of force while permanent clips have over 1.1 N of force [5]. Excessive force or scissoring (misalignment of the blades of the clip) are common problems that can lead to tearing of the artery and intraoperative catastrophe [6]. The shape of the clip is another important component of a clip's function. The exact specifications of the occlusion as well as the method for accessing the artery determine the clip shape required for a given surgery. In some circumstances, fenestrated clips, those with a round opening, are required for allowing passage of an adjacent artery or nervous system tissue (such as a nerve) that should not be clipped [7]. Fenestrated clips can be particularly helpful in more dense regions of brain vasculature or complex aneurysmal circulation.

Aneurysm clip manufacturing is a complicated and labor-intensive process in order to ensure that clips which interact with regions of the brain are of the highest biocompatible standards. Two of the most common aneurysm clip systems are Sugita Bridge Wire (Mizuho Corporation, Tokyo, Japan) and Yasargil (Aesculap AG, Tuttlingen, Germany), the latter of which is shown in Fig. 1. Production of Yasargil clips involves 30 distinct steps and requires more than 70% of the work to be performed manually under a microscope [8]. After production, each clip is checked multiple times for closing force and surface finish. Multiple types of clips are then distributed in packages so the surgeon can later decide which stock clip is best suited for the task.

Despite a large repertoire of clip variations available to surgeons, many procedures potentially require application of multiple different clips for a successful surgery. This is due to the inherent individuality of a given patient's anatomy, with unique vasculature and nerve architecture surrounding an aneurysm conferring different geometries and orientations. Recent advances in medical imaging such as digital subtraction angiography to elucidate vascular anatomy [9] coupled with the development of advanced fabrication techniques like metal three-dimensional (3D) printing [10,11], present an opportunity to create custom and patient-specific aneurysm clips. Custom clips could reduce the number of clips required for a complex case and reduce surgery time and potential risks of complications. Furthermore, the size, complexity, uniqueness, and cost of these parts make them ideal candidates for metal 3D printing.

However, to the best of our knowledge, no analysis of the additive manufacturing of custom metal clips has been conducted, including the challenges one would face in producing these small and complex parts. Presented here is such an investigation of these 3D metal printing challenges as they apply to the manufacturing of aneurysm clips. Two potential clip designs (fenestrated and unfenestrated), were printed on a state-of-the-art metal 3D printer. Different support structures were investigated and the clips themselves were analyzed for material properties. A discussion of how the process of making a custom clip might work, from patient image to final clip, is also included along with the remaining challenges of a clinically viable strategy of using patient-specific aneurysm clips.

Materials and Methods

The creation of the clips used for this investigation required several steps from design to printing to processing to analysis. These steps are detailed in the rest of the manuscript, but are also summarized in an overall workflow schematic in Fig. 2.

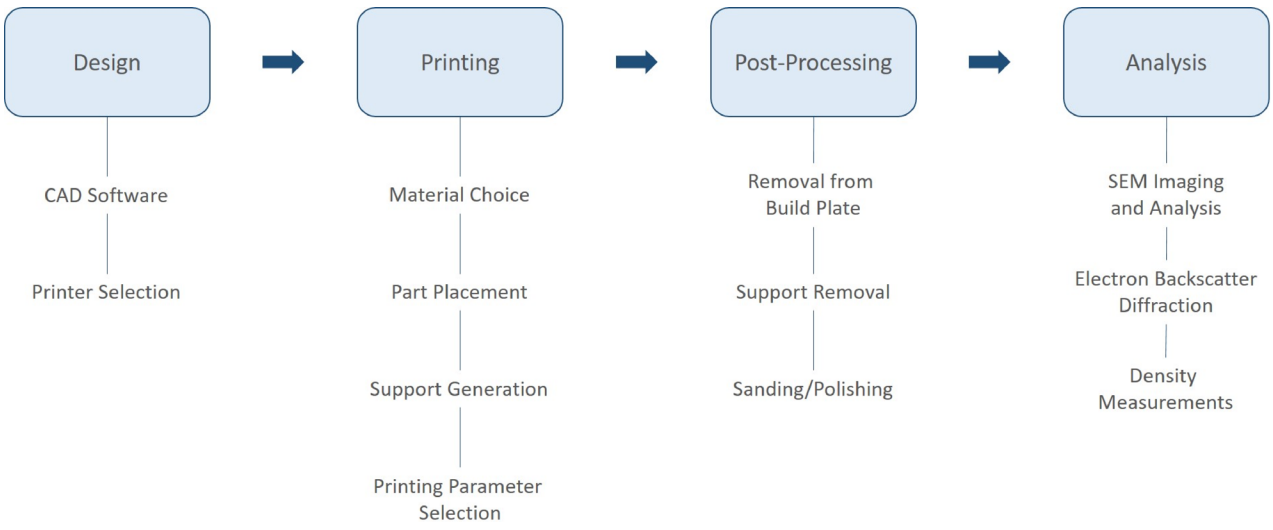

Fig. 2 Schematic of the workflow for the creation of the clips analyzed in this study

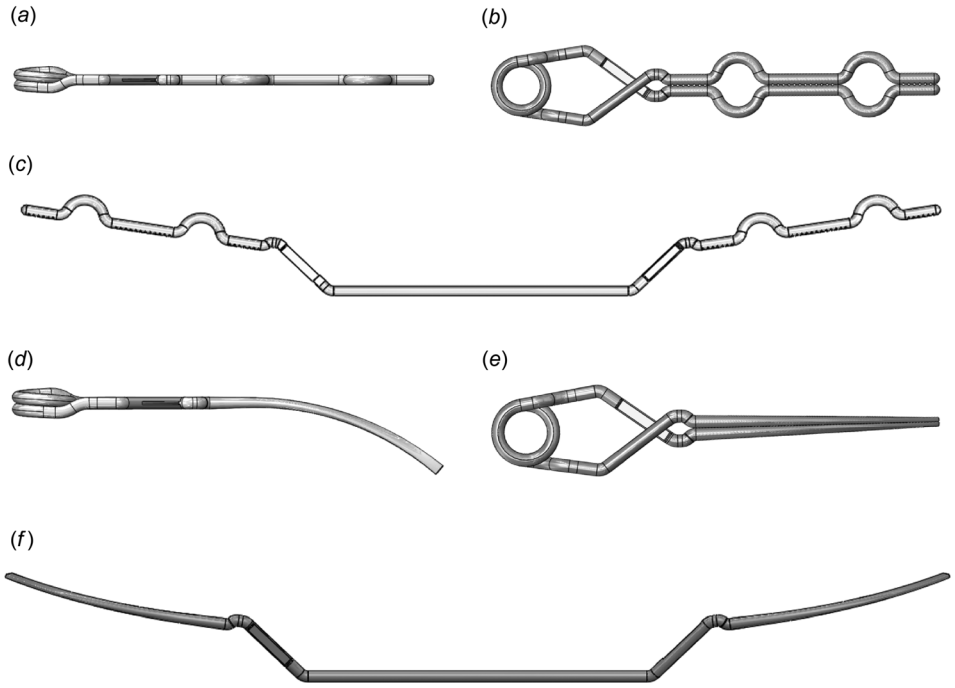

Fig. 3 Designs for a custom fenestrated clip in both bent (*a*) and (*b*) and unbent (*c*) states, along with a curved blade clip design in bent (*d*) and (*e*) and unbent states (*f*)

Aneurysm Clip Design. Two clip designs were created for the purposes of this investigation, one with planar blades and fenestrations to avoid healthy vasculature (Figs. 3(*a*)–3(*c*)), and another design with curved blades but no fenestrations (Figs. 3(*d*)–3(*f*)). The two clip designs were also modeled in two different configuration states corresponding to before or after the coiling process that forms a springy device. Designs were generated using SolidWorks (Dassault Systemes, Velizy-Villacoublay, France), a computer-aided design (CAD) software package. While these designs have features that are found in commercial clips, they are not identical to any particular commercial clip.

The clip design with fenestrations is modeled around a hypothetical situation in which a clip is needed to clamp up to three locations but also avoid two arteries interspersed between the clamp points (Figs. 3(*a*)–3(*c*)). The other tested clip design features long curved blades (Figs. 3(*d*)–3(*f*)), making the design nonplanar. It was used to qualitatively test the capabilities of the EOS M290 printer (EOS, Krailling, Germany) for more complicated clip features, such as an out of plane 3D curve.

Both clip designs were made with dimensions similar to existing commercial clips. The fenestrated test clip was a little longer to account for the multiple fenestrations. An example commercial clip used as the basis for the custom clip design is approximately 25 mm in length, with 1 mm diameter prongs and a max height of about 6 mm. The design with fenestrations in Fig. 3(*b*) is 40 mm in length, with 1 mm diameter prongs and a max height of 7 mm. It should be noted that many of the clips actually printed in this study include a factor of two scale increase in diameter for the initial proof of concept to simplify removal of the part from the build plate and increase the chance of a successful build.

Support Generation. Metal additive manufacturing with a selective laser melting (SLM) process requires additional support structure to secure the part on the substrate, support the weight, and reduce the temperature gradient of the part by transferring the heat of the melt pool to the substrate. Smaller temperature gradients correspond to lower residual stresses in the part which are the primary cause of deformation and warping. Any surface with a normal angled at or greater than a specific range with respect to the build axis requires a support structure to prevent undesirable physical phenomena such as dross. This surface is called the overhang surface and the maximum allowable overhang angle for 316 L austenitic stainless steel (316 L SS) is approximately 45 deg.

Two batches of unbent clips were printed, with a total of five different types of support structures of varying strength, shown in Figs. 4(*a*)–4(*e*). A light support structure in the form of a periodic tree pattern was used as an extreme condition to minimize contact between the supports and actual part to simplify postprocessing (Fig. 4(*a*)), at the cost of limiting heat transfer to the build plate. Increasing in strength, the next type of support structure used featured a line topology (Fig. 4(*b*)) or a reinforced line topology (Fig. 4(*c*)) with added ribs along its length. The final types of support structures used were the meshed block (Fig. 4(*d*)) or solid block (Fig. 4(*e*)) topologies. These should be the strongest supports with the highest heat transfer rates but the most difficult to remove.

Three-Dimensional Metal Printer. An EOS M290 3D metal printer at the UW-Madison Grainger Institute for Engineering was used for the production of the prototype aneurysm clips. The M290 is a laser powder-bed fusion metal printer with a single 400 W Yb fiber laser as the energy source for melting. The $250 \times 250 \times 325\,\text{mm}^3$ build volume contains a build plate upon which a single layer of metal powder is formed. The laser beam is scanned via a galvo process to melt the first cross section of the part (which is typically a cross section of supports) to the underlying build plate. After melting is completed, the build plate is lowered, and a new layer of metal powder is swept across. This process repeats with alternating powder recoating and laser melting of cross section until a final part is formed.

Material Choice. EOS Stainless Steel 316 L metal powder (EOS 9011-0032) designed for use with the EOS M290 Metal 3D Printer was used to print all prototype clips described here. This spherical powder is sold by EOS, the same manufacturer of the metal printer used, and has an average particle diameter of 20 μm. The powder composition was measured with combustion infrared

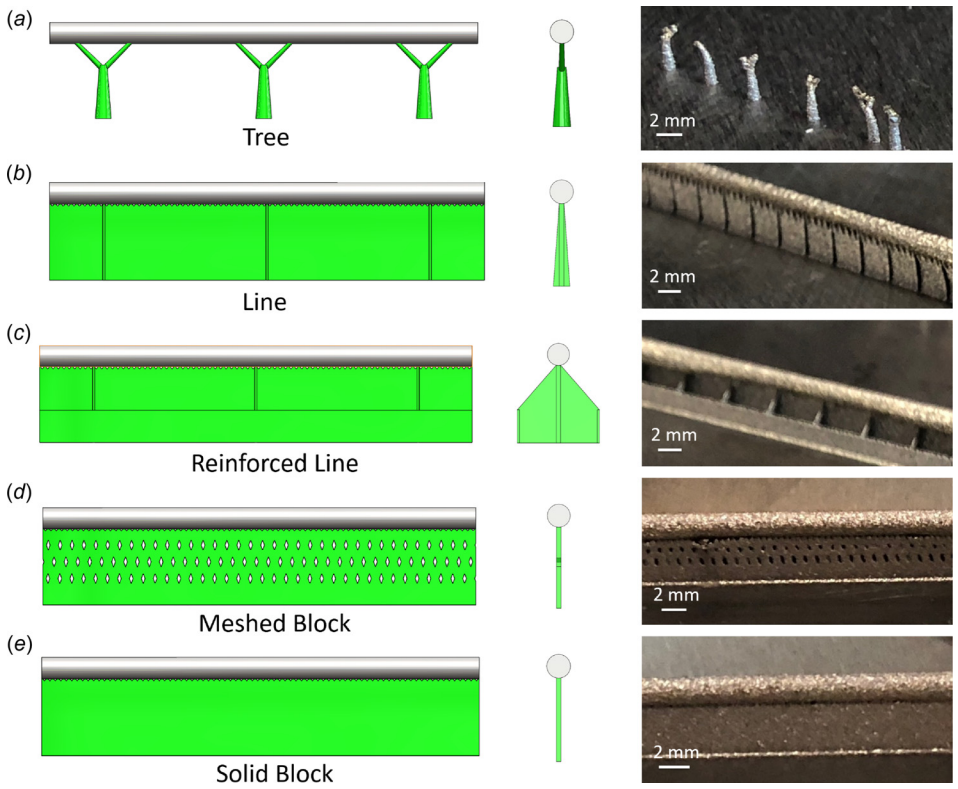

Fig. 4 Support structure designs for aneurysm clips included topologies in the form of trees (*a*), lines (*b*), reinforced lines (*c*), meshed blocks (*d*), and solid blocks (*e*). Front views, side views, and actual printed structures are shown left to right, respectively.

Table 1 Elemental composition of 316 L stainless steel powder used in this study

Powder chemical composition											
Atom	Ni	Cr	Mo	Si	Mn	C	N	Cu	P	O	Fe
% (by wt)	13.94	18.39	2.86	0.30	1.47	0.004	0.065	0.0022	0.017	0.043	Balance

detection (C and S), inert gas fusion (O and N), and direct current plasma emission spectroscopy (all others) and is shown in Table 1.

Most modern aneurysm clips are composed of titanium alloys (Ti–6Al–4V) or Phynox, a cobalt–chromium–nickel alloy, in order to reduce image artifacts and be compatible with followup clinical imaging with magnetic resonance imaging and computed tomography [12]. Type 316 L stainless steel, however, was used for these prototype clips as the powder material was readily available and the literature shows austenitic 300 series stainless steels have been used clinically in the past for many years [13]. Additionally, it was anticipated that 316 L would have a higher chance of providing spring action when compared to 3D-printed titanium, a crucial component of a 3D-printed aneurysm clip. Use of the stainless steel material is only being pursued in this initial proof-of-concept study.

Printing Parameters. This first round of unbent clips was positioned on the build plate at an angle with respect to the recoating blade. It is generally recommended to avoid having a parallel edge of a part aligned with the recoating blade to prevent recoating errors and blade crashes. The part was positioned in a plane parallel and 4 mm above the build plate surface. This kept the total number of layers to print low and subsequently the total time to print low. The parts in a second batch of unbent clips were also positioned to avoid a long parallel part edge with the recoating blade. With regard to part rotation, half of the clips were again printed in a parallel plane 4 mm above the plate surface, while the others were printed with a 90 deg rotation.

The process parameters used with the EOS M290 were different depending on whether the laser was being used to print support material or the actual clip. Table 2 summarizes these parameters for both clip printing and for support printing. For printing the actual clip, a stripe-based scan strategy was employed with a hatch distance of 0.09 mm for printing actual parts. This means that stripes were formed by rastering the laser back and forth, within a given stripe, with a distance of 0.09 mm between passes. The EOS M290 has a nominal beam focus diameter of 0.08 mm and a melt pool of approximately 0.12 mm.

Postprocessing. Multiple postprocessing steps are required after the 3D printing process completes. The part must first be removed from the build plate. The EOS M290 printer fully melts the stock metal powder in both the final part and the support structure, which means that the parts are fully welded to the build plate through the supports. Additively manufactured parts are typically removed from the build plate via a conventional saw or a wire electrical discharge machining (EDM) process. Wire EDM can produce higher precision cuts for delicate parts, but a conventional

Table 2 EOS M290 printing parameters for both clip printing and support printing

Parameter	Setting	Rationale
Printer settings for printing clips		
Laser power	195 W	Suggested by vendor, proved for 99.8% relative density
Layer height	0.02 mm	Extra spatial resolution required for the actual clip
Scan strategy	Stripe-based	Suitable to cover area of small sized components
Hatch distance	0.09 mm	Provided a 25% overlap between beam passes
Laser scan speed	1083 mm/s	Suggested by vendor, proved for 99.8% relative density
Support printer settings		
Laser power	100 W	Suggested by vendor for support printing
Layer height	0.04 mm	Faster and less stringent spatial resolution needed
Scan strategy	Unidirectional	Suitable for supports, where covered area is not a concern
Laser scan speed	675 mm/s	Suggested by vendor for support printing

drop saw was used to remove the printed aneurysm clips in this study due to availability.

Following removal of the clips from the build plate, the excess support material needs to be removed from the part surface. As the aneurysm clips are small, removal of this final layer of supports needs to be performed by hand. A handheld cutting tool (Dremel, Mount Prospect, IL) was used to remove the supports for the clips shown in this study. The Dremel tool was also fitted with sanding and polishing ends of varying grit to smooth the surface of the entire part after the support material had been removed.

Analysis Equipment. Samples for microstructure characterization were prepared by mechanical polishing down to 50 nm colloidal silica solution. Scanning electron microscopy (SEM) analysis was performed in an FEI Helios G4 UX extreme high-resolution field emission SEM. Electron backscatter diffraction (EBSD) maps of the aneurysm clips were collected in the same microscope using an EDAX Hiraki Super EBSD camera and TEAM EBSD data collection software. An accelerating voltage of 30 kV was used with a beam current of 51 nA for EBSD data collection. EBSD maps were indexed and analyzed using EDAX OIM Analysis automated indexing software. The Vickers microhardness was measured using a load of 1 kgf and a loading time of 10 s. A minimum of three indents were performed for each sample. Density was measured using Archimedes method on a Sartorius Practum Precision Weighing Balance with 1 mg readability by immersing samples in Fluorinert FC-40 F9755 liquid.

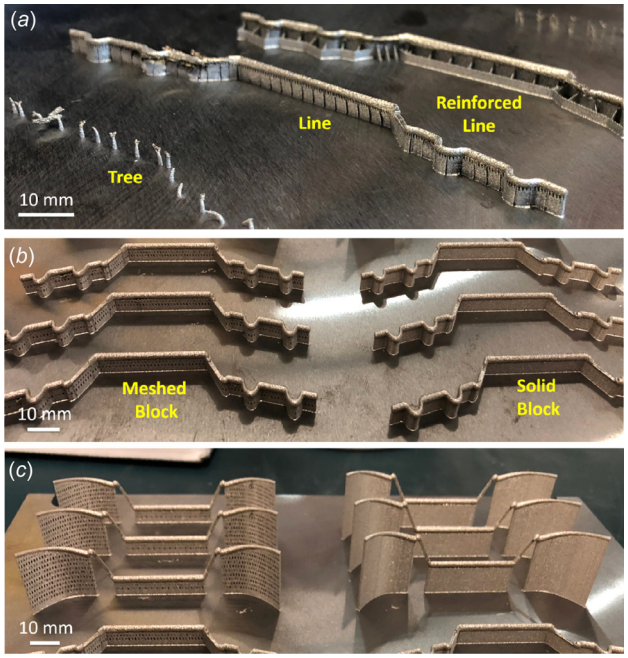

Fig. 5 Aneurysm clips on the build plate after printing. Tree, line, and reinforced line supports were not sufficient to prevent defects (*a*). Meshed block and solid block supports (*b*) produced promising clips. Clips with 3D curved blades were built in panel (*c*).

Results

Build Success With Support Structure Variation. The results of the aneurysm clip printing process with varying support structures are shown in Fig. 5. The tree structure supports had the least contact with the surface of the part, but these clips failed to build, leaving only partially formed sections of clip and severed tree supports on the plate (Fig. 5(*a*)). It is possible that residual stress in the branches exceeded the yield strength of the material, causing the branches to deform and protrude above the print bed. This deformation in turn could have caused collision with the recoater blade and swept away early layers of the clip.

Clips built with line and reinforced line support structures (Fig. 5(*a*)) adhered to the plate but had defects. Clips did not maintain a circular cross section throughout the length of the piece. The surface contact between part and support is limited and may have been insufficient to provide adequate heat conduction from the clip to the build plate, resulting in deformation.

Clips were successfully manufactured without any obvious defects using the meshed block and solid block supports in Fig. 5(*b*). Adequate heat conduction provided by the support structure helped preserve the model's geometry. The curved blade clips shown in Fig. 5(*c*) were successfully printed with both types of block supports and demonstrate the capability of printing more complex out of plane clip designs. The clips in Figs. 5(*b*) and 5(*c*) were subsequently removed from the build plate, a portion of which also had their supports removed. Of the samples with supports removed, one was chosen for SEM analysis and a second was chosen for polishing by hand and bending into a prototype aneurysm clip.

Build Time and Measured Accuracy. The planar fenestrated clips (Fig. 5(*b*)) take approximately 1 h per clip to build, according to the printer planning software. The curved blade clips oriented at 90 deg (Fig. 5(*c*)) required more layers and subsequently more time to build, with a projected build time of approximately 3.5 h per clip. The entire build for all clips in Figs. 5(*b*) and 5(*c*) took approximately 6 h.

Three measurements were taken to assess the deviation of a printed fenestrated clip (Fig. 5(*b*)) from the CAD drawings after the clip has been removed from the build plate. Overall length of the printed part was experimentally measured to be 93.3 mm, compared to the CAD length of 93.5 mm. The maximum height was experimentally measured to be 21.6 mm, compared to the CAD height of 21.5 mm. Finally, the diameter of the center of clip

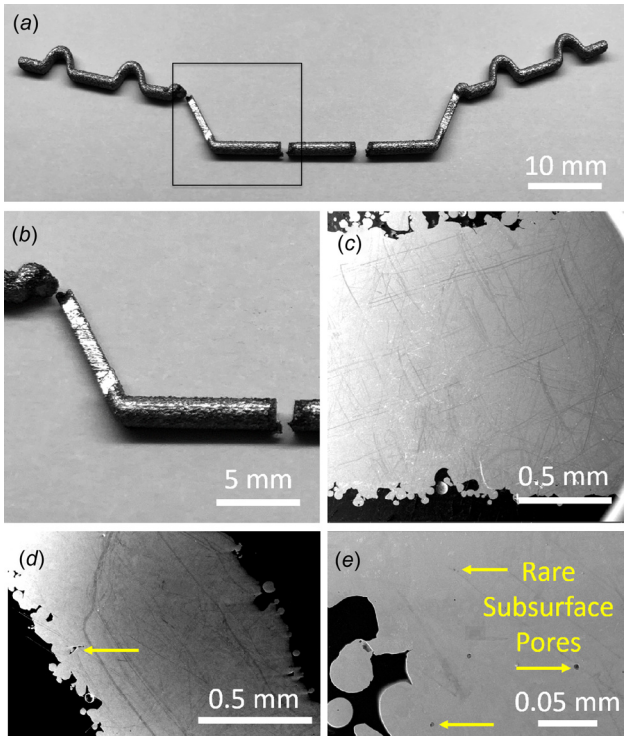

Fig. 6 V-shaped sample taken from the clip (*a*) and (*b*) for SEM imaging. Low porosity observed in thick section (*c*) of sample and thin section (*d*). Close up of rare pores shown in (*e*).

where coiling would occur was experimentally measured to be 2.0 mm, compared to the CAD diameter of 2.0 mm. All three measurements were within ±0.5% of the original design after removal from the build plate. There was some minor warping of the clip after removal from the plate, but was easily corrected by applying slight pressure to bend back to shape. These printed clips have scaled up diameters and are twice as large as the example Yasargil clip with a diameter of 1.0 mm from Fig. 1.

Porosity. Cross-sectional SEM images of a V-shaped sample from a printed aneurysm clip are shown in Fig. 6. The V-shaped sample in Fig. 6(*b*) has a horizontal thick portion and a diagonal thin portion with SEM images shown in Figs. 6(*c*) and 6(*d*), respectively. Solid metal is visible through the images with limited pores, some of which are shown in Fig. 6(*e*). The small rare pores that exist lie near the surface of the clip and may be able to be removed with further postprocessing, as porosity can have detrimental effects on fatigue [14]. In the cross sections shown, the build axis is out of the page. Samples were not sanded or polished beyond the cutting surface for imaging, so are representative of as-printed structures. The surface is much too rough for use without postprocessing, but sanding, mechanical polishing, and electropolishing could remove the roughness observed.

Hardness and Density. Vickers microhardness testing [15] was performed with 1 kgf (HV1) in the V-shaped sample from Fig. 6(*b*) and averaged 213±7 HV1. Microhardness results are comparable to other 316 L additive manufacturing steels. There is some anisotropy with slightly higher hardness in the cross section sample. Additionally, the aneurysm clips printed out of 316 L stainless steel were measured to have a density of 7.9 g/cc using the Archimedes method, close to standard density of 8.0 g/cc in the literature.

Grain Morphology In-Plane. An EBSD orientation map and inverse pole figure triangle of randomly selected points in Fig. 7 shows some <001> and <011> texture and depletion in <111> texture along the build direction. This is a common observation for SLM-produced austenitic stainless steels which is likely caused by a combination of <100> crystal growth along the direction of maximum thermal gradient and specific melt pool morphologies [14,16–19]. Anisotropy in the grain orientation can have effects on both yield strength and fatigue strength for 316 L printed parts. When compared to wrought 316 L, yield strength increases but fatigue strength decreases, with particularly worse fatigue strength in the build direction [20]. The fenestrated aneurysm clips were built such that the coil bending would occur within the build plane, to minimize the chances of poor fatigue strength causing problems with coil formation.

Phase maps were also used to observe the presence of austenite or ferrite within the 3D-printed clip. No ferrite was found. Ferrite within the clips would lead to increased artifacts for magnetic resonance imaging imaging postsurgery.

Prototype Clip and Clamping Force. One printed fenestrated clip from Fig. 5(*b*) was chosen for further postprocessing and coiling into a prototype aneurysm clip, shown in Fig. 8. After supports were removed using a Dremel rotary tool in a vice, sanding wheel attachments of successively higher grit were used to smooth the

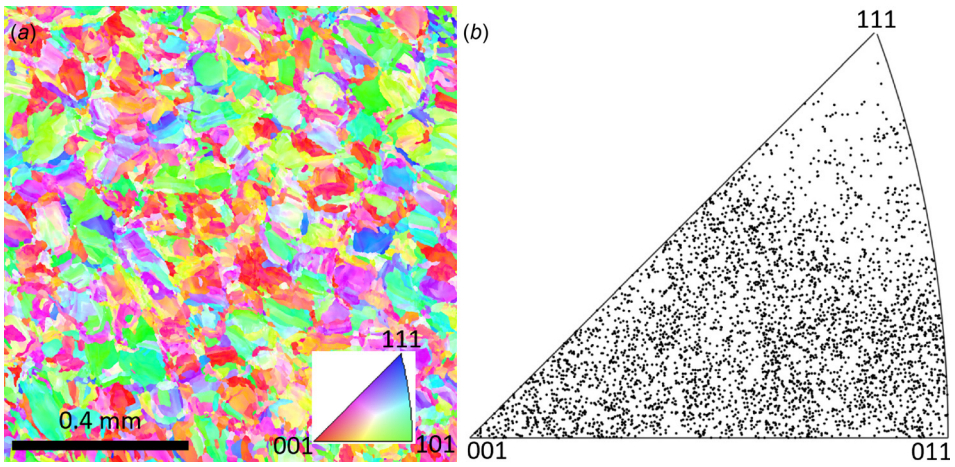

Fig. 7 (*a*) EBSD orientation map of the sample in Fig. 6(*b*) colorized according to the crystal orientation aligned with the build direction (direction perpendicular to the plane of the image). (*b*) Orientation of 4000 randomly selected points from the EBSD map according to the build direction (direction perpendicular to the plane of the image).

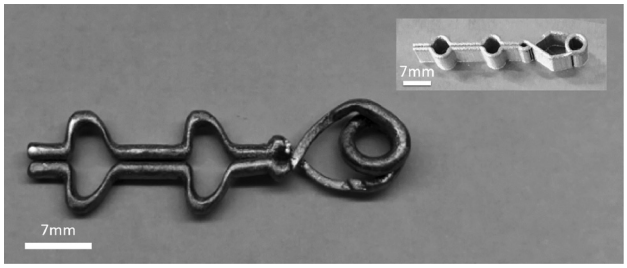

Fig. 8 Three-dimensional printed custom fenestrated aneurysm clip after support removal, sanding, and manual coiling. Also shown is another clip printed directly in a coiled state (inset).

surface. The raw printed surface is naturally very coarse (Fig. 6) but is easily removed with an abrasive sanding wheel. A final pass with a polishing attachment was used on the clip. Although the surface was noticeably improved with the mechanical abrasive tools, it is expected that a clinical version would need further surface processing in the form of electropolishing to yield a sufficiently smooth aneurysm clip.

The clamping force was measured as a function of clip opening distance with the measurement point approximately 6 mm from the end of the tip, at the apex of the most distal fenestration. Data were very noisy and oscillatory, likely due to a combination of movement of the clip, sliding of the measurement point, imperfect coiling, and possibly vibration of the setup. A coarse average was performed to show an approximate force of 1 N with a clip separation of 1.5 mm. This is less than the clamping force of 1.5–3 N typically seen in an aneurysm clip at the same measurement point and clip separation [12].

Fenestrations do not appear as perfect half-circles in Fig. 8 due to the factor of two scaling applied in the plane transverse to the long axis of the clip. Although the transformation did not preserve shape, the printed clip shape matches the scaled digital model.

Discussion

It was unclear prior to this experiment whether a 3D-metal printed clip would readily bend without fracture, but the as-produced material easily yielded under stress to form a coil shape with a springy nature. The prototype clip was bent by hand, however, and did not achieve an optimal coil design, likely causing difficulties with the closing force measurements. A coiling process and machine ideally should be setup to more uniformly and predictably bend the polished clip into its final shape in order to achieve better clamping characteristics. The printing parameters and scan strategy are expected to have an effect on the mechanical properties of the clips, including ductility, fatigue strength, yield strength, and hardness, but further research would be needed in order to optimize the complex set of laser scanning and environmental factors for a given application. Research is ongoing in microstructure control in metal additive manufacturing and simulation to try to predict how some of these parameters affect the final part [21,22].

Additional postprocessing steps considered but not employed in this presented work are a final polishing treatment, to further improve the surface smoothness, and heat treatment of the part. Although the determination of what the optimal surface finish for an aneurysm clip should be in general does not appear to be well defined in the literature even for existing clips, there are many commercial options for polishing additively manufactured parts. Mechanical polishing with fine abrasives, bead blasting, laser polishing [23], ultrasonic cavitation [24], and electrochemical [25] options are all possible means of polishing the aneurysm clips, and other studies have examined biocompatibility of additively manufactured implants relative to surface finish, porosity, and other mechanical properties with promising results [10,26,27]. Some biocompatibility studies have also discussed advantages to implants with surfaces that are not smooth and are instead porous [28,29]. The clip surfaces that clamp down on the aneurysm also typically have further surface modifications formed through metal stamping to increase the frictional coefficients in order to prevent the clip from slipping off, although recent research has shown that a laser processing machine can be used instead to increase the frictional coefficient by forming grooved surfaces with a channel width of 30 μm and pitch of 40 μm [30]. With additive manufacturing, it may even be possible to directly print the clamp surfaces with grooves to prevent slipping of the aneurysm clips, although further research would be required. Heat treatment can be employed while the part is still attached to the build plate to relieve stress in the clip, helping to prevent warpage during removal from the build plate and further tailor the microstructure. Removal of supports was performed by hand but could be automated with a robotic arm and rotary sanding tools in combination with various imaging modalities to speed up the process in a clinical workflow. Although this initial clip required a large amount of manual postprocessing, the process could be further refined. As an example, the clips could be removed quickly with minimal distortion using an EDM process, then supports removed using an automated robotic arm with a rotary tool to follow the preprogrammed CAD model, then polished using batched techniques like electropolishing, with a final coiling step in an automated machine specifically built to produce a consistent coil and clamping force.

For creating custom aneurysm clips, the size and complexity of the clips themselves make them a great candidate for metal 3D printing. Furthermore, their 3D printing time of 1–3 h (depending on clip shape) is appropriate to fit into current clinical workflows. For these reasons, and despite the technical challenges remaining, the creation of custom aneurysm clips on a patient-specific basis is a promising idea that could greatly reduce the number of clips needed, reduce surgery time, and improve patient outcomes.

However, before custom clips can be adopted clinically, an overall clinical workflow would need to be developed, as physically printing the clips is only one part of a more complex and necessary workflow (Fig. 9). While metal printing can be used to replicate currently available aneurysm clip designs, a large advantage of the metal printing approach is printing from image-based designs for a given patient. To realize this potential, before printing, patients would need to be imaged in order to reveal the key anatomical structures (vascular and nervous system tissue) surrounding an aneurysm. Models of the ideal custom clip could then be created using the anatomy as a guide. Printing of the custom clip results in a part that would need extensive postprocessing to remove it from the build plate, polish it, bend it into the correct shape, and test its functionality. Only after all these postprocessing steps are complete would a final clip be ready for clinical use. Future studies will need to investigate the utility of this including working with real image data, but the potential of a personalized clip in geometry and fit could have advantages for patient care and outcome.

Manufacturing Process With Hybrid Clip. These initial experiments with metal additive manufacturing of aneurysm clips were conducted with clip models that were in an unbent state and manually coiled into a shape that can produce spring force. Automating the coiling process for custom clinical clips in this fashion could prove challenging, however. A second option is envisioned as another means for producing patient-specific aneurysm clips that is a hybrid approach between conventional manufacturing and additive manufacturing in order to minimize the difficulty of printing a piece that functions well as a spring.

In this second approach, the back end of the clip with the coil that produces a spring force would be produced from an ordinary wire alloy and twisted via traditional techniques to provide the correct clamping force. The custom end pieces that clamp together with multiple curves and fenestrations would then be produced

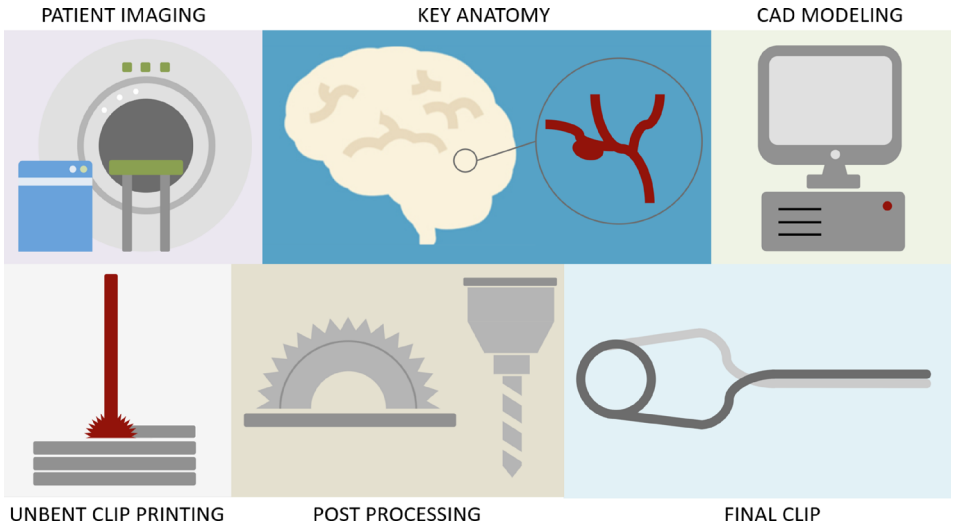

Fig. 9 Workflow for creating custom aneurysm clips with additive manufacturing

per patient with a 3D metal printer and welded to the coil piece. Care would need to be taken to limit heat transfer to the coil in order to not heat treat this section, as doing so could affect the closing force. In this second method of production, the coils could be mass produced in a small number of sizes, and the clip ends that are based on 3D scans of the patient anatomy would be additively manufactured and attached prior to surgery.

Future Work. One of the biggest challenges to the additive manufacturing of aneurysm clips that became apparent from these experiments is finding a way to minimize the postprocessing involved, including build plate removal, support removal, polishing, and bending to the final shape. Support removal was done by hand in a tedious fashion, so there is much room for improvement in refining the support structure to simplify the process. The bending of the final aneurysm clip was also done by hand, but could be improved by building a form to coil the clips more efficiently. In addition to efforts on streamlining these postprocessing steps, future experiments will focus on reducing the size of the additively manufactured clips and on material properties. Due to the current clinical acceptance and compatibility with clinical MRI, production of titanium aneurysm clips should be attempted and compared to what we learned from the 316 L stainless steel prototypes. Optimizing choice of materials, clip configurations, and patient anatomy customization processes are all required before rigorous clinical testing would enable application of this strategy in advancing neurosurgical care of patients with cerebral aneurysms.

Conclusion

Metal additive manufacturing was investigated as a possible means of production for patient-specific aneurysm clips out of 316 L stainless steel powder. The various steps required to produce a clip with a powder bed–based 3D metal printer were studied including CAD design, support structure design, the printing process, and postprocessing. Sturdy block type support structures were found to be necessary for printing an aneurysm clip, despite the small size of the part but required extensive manual postprocessing to remove the supports from the clip. SEM images showed low porosity within the clips and density was measured to be similar to wrought steel. EBSD inverse pole maps showed preferred grain growth along the build direction, which may have implications for fatigue strength for a springy clip. Phase maps showed only austenite in the clips. A prototype custom 316 L stainless steel clip was printed, bent to shape, and polished, demonstrating that additive manufacturing is a promising technique for the creation of custom medical devices, albeit with significant challenges remaining for further research and potential clinical translation.

Acknowledgment

The authors would like to thank Max Roth for help in SEM sample preparation.

Funding Data

- National Science Foundation (NSF) through the University of Wisconsin Materials Research Science and Engineering Center (DMR-1720415), NSF-DMREF under Grant No. DMR-1728933 (Funder ID: 10.13039/501100008982).
- Morgridge Institute for Research with the University of Wisconsin—Madison (Grant No. UW2020; Funder ID: 10.13039/100007015).
- Wisconsin Alumni Research Foundation (Funder ID: 10.13039/100001395).

Nomenclature

CAD = computer aided design
EBSD = electron backscatter diffraction
SEM = scanning electron microscope
SLM = selective laser melting
SS = stainless steel

References

[1] Miller, T. S., Altschul, D., Baxi, N., Farinhas, J., Pasquale, D., Burns, J., Gordon, D., Bello, J., Brook, A., and Flamm, E., 2017, "Comparison of the Prevalence of Ruptured and Unruptured Cerebral Aneurysms in a Poor Urban Minority Population," J. Stroke Cerebrovasc. Dis., **26**(10), pp. 2287–2293.
[2] Feigin, V. L., Rinkel, G. J. E., Lawes, C. M. M., Algra, A., Bennett, D. A., Van Gijn, J., and Anderson, C. S., 2005, "Risk Factors for Subarachnoid Hemorrhage: An Updated Systematic Review of Epidemiological Studies," Stroke, **36**(12), pp. 2773–2780.
[3] D'Souza, S., 2015, "Aneurysmal Subarachnoid Hemorrhage," J. Neurosurg. Anesthesiol., **27**(3), pp. 222–240.
[4] Ljunggren, B., Saveland, H., Brandt, L., Kagstrom, E., Rehncrona, S., and Nilsson, P.-E., 1983, "Temporary Clipping During Early Operation for Ruptured Aneurysm: Preliminary Report," Neurosurgery, **12**(5), pp. 525–530.
[5] Ooka, K., Shibuya, M., and Suzuki, Y., 1997, "A Comparative Study of Intracranial Aneurysm Clips: Closing and Opening Forces and Physical Endurance," Neurosurgery, **40**(2), pp. 318–323.
[6] Horiuchi, T., Hongo, K., and Shibuya, M., 2012, "Scissoring of Cerebral Aneurysm Clips: Mechanical Endurance of Clip Twisting," Neurosurg. Rev., **35**(2), pp. 219–224.

[7] Sugita, K., Kobayashi, S., Kyoshima, K., and Nakagawa, F., 1982, "Fenestrated Clips for Unusual Aneurysms of the Carotid Artery," J. Neurosurg., **57**(2), pp. 240–246.
[8] Aesculap, 2017, "Yasargil Aneurysm Clip System," Aesculap AG, Tuttlingen, Germany, accessed Jan. 13, 2019, https://www.bbraun.com.au/en/products/b/yasargil-aneurysmclipsystem. html
[9] Chen, W., Xing, W., Peng, Y., He, Z., Wang, C., and Wang, Q., 2016, "Diagnosis and Treatment of Intracranial Aneurysms With 320-Detector Row Volumetric Computed Tomography Angiography," World Neurosurg., **91**, pp. 347–356.
[10] Sing, S. L., An, J., Yeong, W. Y., and Wiria, F. E., 2016, "Laser and Electron-Beam Powder-Bed Additive Manufacturing of Metallic Implants: A Review on Processes, Materials and Designs," J. Orthop. Res., **34**(3), pp. 369–385.
[11] Pucci, J. U., Christophe, B. R., Sisti, J. A., and Connolly, E. S., 2017, "Three-Dimensional Printing: Technologies, Applications, and Limitations in Neurosurgery," Biotechnol. Adv., **35**(5), pp. 521–529.
[12] Nagatani, T., Shibuya, M., Ooka, K., Suzuki, Y., Takayasu, M., and Yoshida, J., 1998, "Titanium Aneurysm Clips: Mechanical Trial Characteristics and Clinical Trial," Neurol. Med. Chir., **38**, pp. 39–44.
[13] McFadden, J. T., 2012, "Magnetic Resonance Imaging and Aneurysm Clips," J. Neurosurg., **117**(1), pp. 1–11.
[14] Song, B., Zhao, X., Li, S., Han, C., Wei, Q., Wen, S., Liu, J., and Shi, Y., 2015, "Differences in Microstructure and Properties Between Selective Laser Melting and Traditional Manufacturing for Fabrication of Metal Parts: A Review," Front. Mech. Eng., **10**(2), pp. 111–125.
[15] Tabor, D., 1970, "The Hardness of Solids," Rev. Phys. Technol., **1**(3), pp. 145–179.
[16] Song, M., Wang, M., Lou, X., Rebak, R. B., and Was, G. S., 2019, "Radiation Damage and Irradiation-Assisted Stress Corrosion Cracking of Additively Manufactured 316 L Stainless Steels," J. Nucl. Mater., **513**, pp. 33–44.
[17] Sun, Z., Tan, X., Tor, S. B., and Chua, C. K., 2018, "Simultaneously Enhanced Strength and Ductility for 3D-Printed Stainless Steel 316 L by Selective Laser Melting," NPG Asia Mater., **10**(4), pp. 127–136.
[18] Wang, X., Muñiz-Lerma, J. A., Sanchez-Mata, O., Attarian Shandiz, M., Brodusch, N., Gauvin, R., and Brochu, M., 2019, "Characterization of Single Crystalline Austenitic Stainless Steel Thin Struts Processed by Laser Powder Bed Fusion," Scr. Mater., **163**, pp. 51–56.
[19] Andreau, O., Koutiri, I., Peyre, P., Penot, J. D., Saintier, N., Pessard, E., De Terris, T., Dupuy, C., and Baudin, T., 2019, "Texture Control of 316 L Parts by Modulation of the Melt Pool Morphology in Selective Laser Melting," J. Mater. Process. Technol., **264**, pp. 21–31.
[20] Mower, T. M., and Long, M. J., 2016, "Mechanical Behavior of Additive Manufactured, Powder-Bed Laser-Fused Materials," Mater. Sci. Eng. A, **651**, pp. 198–213.
[21] Xu, W., Lui, E. W., Pateras, A., Qian, M., and Brandt, M., 2017, "In Situ Tailoring Microstructure in Additively Manufactured Ti-6Al-4V for Superior Mechanical Performance," Acta Mater., **125**, pp. 390–400.
[22] Zinovieva, O., Zinoviev, A., and Ploshikhin, V., 2018, "Three-Dimensional Modeling of the Microstructure Evolution During Metal Additive Manufacturing," Comput. Mater. Sci., **141**, pp. 207–220.
[23] Tian, Y., Gora, W. S., Cabo, A. P., Parimi, L. L., Hand, D. P., Tammas-Williams, S., and Prangnell, P. B., 2018, "Material Interactions in Laser Polishing Powder Bed Additive Manufactured Ti6Al4V Components," Addit. Manuf., **20**, pp. 11–22.
[24] Tan, K. L., and Yeo, S. H., 2017, "Surface Modification of Additive Manufactured Components by Ultrasonic Cavitation Abrasive Finishing," Wear, **378–379**, pp. 90–95.
[25] Urlea, V., and Brailovski, V., 2017, "Electropolishing and Electropolishing-Related Allowances for Powder Bed Selectively Laser-Melted Ti-6Al-4V Alloy Components," J. Mater. Process. Technol., **242**, pp. 1–11.
[26] Sidambe, A. T., 2014, "Biocompatibility of Advanced Manufactured Titanium Implants-A Review," Materials (Basel), **7**(12), pp. 8168–8188.
[27] Kong, D., Ni, X., Dong, C., Lei, X., Zhang, L., Man, C., Yao, J., Cheng, X., and Li, X., 2018, "Bio-Functional and Anti-Corrosive 3D Printing 316 L Stainless Steel Fabricated by Selective Laser Melting," Mater. Des., **152**, pp. 88–101.
[28] Yang, F., Chen, C., Zhou, Q., Gong, Y., Li, R., Li, C., Klämpfl, F., Freund, S., Wu, X., Sun, Y., Li, X., Schmidt, M., Ma, D., and Yu, Y., 2017, "Laser Beam Melting 3D Printing of Ti6Al4V Based Porous Structured Dental Implants: Fabrication, Biocompatibility Analysis and Photoelastic Study," Sci. Rep., **7**, pp. 1–12.
[29] Tan, X. P., Tan, Y. J., Chow, C. S. L., Tor, S. B., and Yeong, W. Y., 2017, "Metallic Powder-Bed Based 3D Printing of Cellular Scaffolds for Orthopaedic Implants: A State-of-the-Art Review on Manufacturing, Topological Design, Mechanical Properties and Biocompatibility," Mater. Sci. Eng. C, **76**, pp. 1328–1343.
[30] Nitta, I., Tsukiyama, Y., Nomura, S., and Takatsu, N., 2016, "Frictional Characteristics of Clamp Surfaces of Aneurysm Clips Finished by Laser Processing," J. Adv. Mech. Des. Syst. Manuf., **10**(2), pp. 1–12.